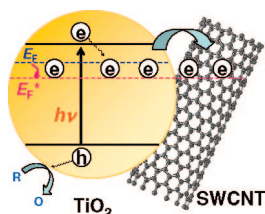# Electron Storage in Single Wall Carbon Nanotubes. Fermi Level Equilibration in Semiconductor–SWCNT Suspensions

Anusorn Kongkanand and Prashant V. Kamat*

Radiation Laboratory, Departments of Chemistry & Biochemistry and Chemical & Biomolecular Engineering, University of Notre Dame, Notre Dame, Indiana 46556-0579

The unique electrical and electronic properties, wide electrochemical stability window, and high surface area render single wall carbon nanotubes (SWCNTs) as scaffolds to anchor light-harvesting assemblies.[1–5] The semiconducting SWCNTs have been shown to play an important role in improving the performance of organic photovoltaic cells[6] and fuel cells.[7,8] They also display photoelectrochemical effects under visible light irradiation.[9,10] TiO_2 and ZnO nanowires and nanotubes have also been employed in dye-sensitized solar cells.[11–15] An effort was recently made to organize semiconductor nanoparticles (ZnO and CdS quantum dots) on SWCNTs and utilize these composites as light harvesting assemblies.[4] An electron-transfer pathway was proposed to explain the emission quenching of these semiconductor nanoparticles by SWCNT. An illustration of the electron transfer between a photoexcited semiconductor nanoparticle and SWCNT is presented in Scheme 1.

Design of nanotube or nanowire architecture provides a convenient way to direct the flow of photogenerated charge carriers.[11,16,17] Use of SWCNT networks as conducting scaffolds has been proposed to boost the photoelectrochemical performance of nanostructure semiconductor-based solar cells.[18] To date the electron-

ABSTRACT The use of single wall carbon nanotubes (SWCNTs) as conduits for transporting electrons in a photoelectrochemical solar cell and electronic devices requires better understanding of their electron-accepting properties. When in contact with photoirradiated TiO_2 nanoparticles, SWCNTs accept and store electrons. The Fermi level equilibration with photoirradiated TiO_2 particles indicates storage of up to 1 electron per 32 carbon atoms in the SWCNT. The stored electrons are readily discharged on demand upon addition of electron acceptors such as thiazine and oxazine dyes (reduction potential less negative than that of the SWCNT conduction band) to the TiO_2–SWCNT suspension. The stepwise electron transfer from photoirradiated TiO_2 nanoparticles → SWCNT → redox couple has enabled us to probe the electron equilibration process and determine the apparent Fermi level of the TiO_2–SWCNT system. A positive shift in apparent Fermi level (20–30 mV) indicates the ability of SWCNTs to undergo charge equilibration with photoirradiated TiO_2 particles. The dependence of discharge capacity on the reduction potential of the dye redox couple is compared for TiO_2 and TiO_2–SWCNT systems under equilibration conditions.

KEYWORDS: electron storage · single wall carbon nanotubes · semiconductor nanoparticles · electron transfer · charge equilibration

accepting and -transport properties of SWCNTs have been demonstrated by the increase in photocurrent or photoconductivity of semiconductor–SWCNT composites,[2–5] yet little effort has been made to estimate the electron-storage property of SWCNTs in a quantitative manner. Unlike fullerenes (*e.g.*, C_{60}), the reduced SWCNT has no detectable absorption in the visible range. This makes direct spectroscopic characterization of the electrons residing within the SWCNT rather difficult. Electrochemical studies have noted charging effects associated with electron storage.[19–21] Storage of such electrons has been shown to affect the G-band of the resonance Raman spectrum.[22–25] Preliminary study of electron transfer between methyl viologen radical and SWCNT has demonstrated the ability to capture electrons (one electron per ~100 carbon atoms of SWCNT) in suspensions.[26] Photochemical studies have also prompted electron transfer from

Scheme 1. Photoinduced electron transfer between an excited semiconductor nanoparticle and SWCNT and charge equilibration.

excited chromophores (*e.g.*, porphyrins) to SWCNT and generation of sensitized photocurrent in a photoelectrochemical cell.[27–29] Two obvious questions arise from these studies: What factors control the electron-accepting property of SWCNTs and how does the electron storage influence the overall energetics of the semiconductor–SWCNT composites?

We report here the charge equilibration processes between photoirradiated TiO$_2$ nanoparticles and SWCNT, and TiO$_2$–SWCNT composite and a redox couple. The stepwise electron transfer from TiO$_2$ to SWCNT and from SWCNT to redox couple is monitored systematically by following the absorption characteristics of trapped electrons and the reduced form of the redox couple, respectively. The results that describe the influence of Fermi level equilibration on the overall electron-transfer yield and the photoelectrochemical performance of nanostructured TiO$_2$ and TiO$_2$–SWCNT film are presented here.

RESULTS AND DISCUSSION

Electron Transfer between UV-Irradiated TiO$_2$ and SWCNT. When TiO$_2$ nanoparticles are subjected to bandgap excitation ($\lambda < 380$ nm), they undergo charge separation (reactions 1 and 2). Whereas a majority of these charge carriers recombine, a fraction of these charge carriers get trapped at the surface vacancies. As the photogenerated holes (h$_{VB}$) are scavenged by ethanol, the electrons get trapped at Ti^{4+} centers.

$$TiO_2 + h\nu \rightarrow TiO_2(e + h) \qquad (1)$$

$$TiO_2(e + h) + C_2H_5OH \rightarrow TiO_2(e_t) + C_2H_5O^\bullet \qquad (2)$$
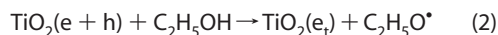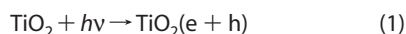
The trapping of electrons (e$_t$) at the Ti^{4+} center has been extensively investigated using transient absorption spectroscopy,[30,31] microwave conductivity,[32–34] and EPR techniques.[35–37] The spectrum a in Figure 1
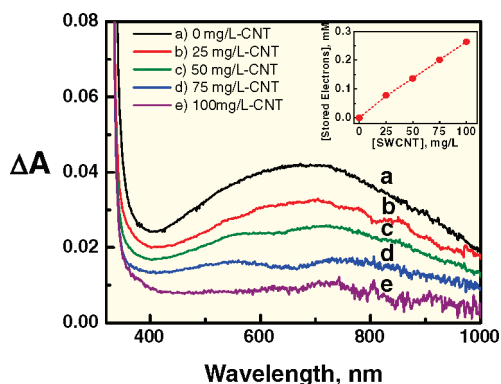

Figure 1. Absorption spectra of deaerated TiO$_2$ particle suspension in ethanol after UV irradiation for 10 min. (a) Before addition of SWCNT suspension; (b–e) upon addition of varying amounts of SWCNT suspension under N$_2$ atmosphere. A non-irradiated TiO$_2$–SWCNT suspension with matching concentration was used as a reference. Inset shows the amount of electrons transferred from TiO$_2$ to SWCNT as a function of SWCNT concentration.

shows the absorption change associated with the steady-state UV irradiation ($\lambda > 300$ nm) of TiO$_2$ colloids. The blue coloration associated with broad absorption in the red region (absorption maximum ~650 nm) represents trapped electrons. These trapped electrons remained stable as long as we maintained a nitrogen atmosphere. On the basis of the extinction coefficient of 760 M^{-1} cm^{-1} (at 650 nm) and the magnitude of the absorption change, we estimate about 3770 electrons stored per TiO$_2$ particle of average diameter 12 nm. See Supporting Information for the procedure employed for the estimation of electrons. This value is consistent with the estimate obtained with the density of electronic states, n_C, available in the conduction band of TiO$_2$.[38]

Addition of deaerated SWCNT suspension to the UV-irradiated TiO$_2$ suspension under inert (nitrogen or argon) atmosphere causes the blue color to decrease. Because the electrons stored in SWCNT do not possess any characteristic absorption features in the visible region, we probed the behavior of electron equilibration in the TiO$_2$–SWCNT system by following the changes in the absorption of trapped electrons. The absorption spectra b–e in Figure 1 show the spectral changes associated with increasing amount of SWCNT. This decrease in the absorbance represents a decrease of trapped electrons in TiO$_2$ as they are transferred to SWCNT. At a concentration of 100 mg/L SWCNT we observe complete disappearance of the 650 nm absorption band, thus indicating complete transfer of electrons to SWCNT. The observed electron transfer from excited TiO$_2$ into SWCNT is similar to the results obtained with other electron acceptors such as C$_{60}$,[31] thiazine dyes,[39,40] and gold nanoparticles.[41,42] The transfer of electrons represents charge equilibration between the two semiconductor systems having different Fermi levels.[42]

If indeed the decrease in the absorbance at 650 nm corresponds to the fraction of the electrons transferred to SWCNT, we should be able to obtain a quantitative estimate of the number of electrons stored in SWCNT. The electrons stored in SWCNT under equilibration conditions were estimated from the absorbance decrease and the extinction coefficient of trapped electrons in TiO$_2$ (760 M^{-1} cm^{-1}). The inset in Figure 1 shows the concentration of electrons stored in SWCNT as a function of SWCNT concentration. The ability of SWCNT to accept electrons in a quantitative manner is evident from the linear increase in electron storage with increasing concentration of SWCNT. From the slope of this plot, we estimate the concentration of stored electrons per milligram of SWCNT. On the basis of the molar concentrations of electrons transferred and molar concentration of carbon in the SWCNT suspension, we obtain a storage value of 0.26 mM of electron per 100 mg/L SWCNT (or 8.3 mM carbon). The ratio of the two concentration values corresponds to 1 electron for 32
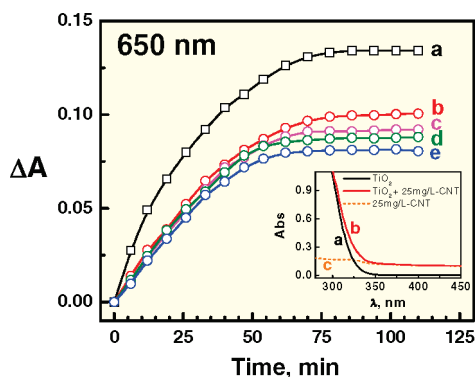
Figure 2. Absorbance change at 650 nm following the steady-state UV photolysis of deaerated suspensions of TiO_2 + SWCNT in ethanol. The SWCNT concentrations were (a) 0, (b) 25, (c) 50, (d) 75, and (e) 100 mg/L. The inset compares the absorbance spectra of (a) TiO_2, (b) TiO_2 + 25 mg/L SWCNT, and (c) 25 mg/L SWCNT in ethanol.

carbon atoms in the nanotubes. The electron storage value achieved for the TiO_2–SWCNT system is better than that obtained with methyl viologen radical (MV$^{+\bullet}$) as the electron donor (1 electron per 100 carbon atoms).[26] As will be discussed in the following sections, the electrons stored in SWCNT can be readily titrated on demand using a redox couple having lower reduction potential.

The SWCNT bundles are known to possess high electron-storage capacity and are often referred to as supercapacitors.[19,21,43] For example, by charging the SWCNT bundles at ~−3.1 V, an intercalation of Li$^+$ ions with a capacity of one Li$^+$ ion per two carbon atom ($Li_{0.5}C$ at 0 V vs Li/Li$^+$) has been reported.[44,45] The electron storage in the present experiments is achieved using photoirradiated TiO_2 colloids under equilibration conditions. Obviously, the driving force in the TiO_2 sys-

tem ($E_{CB} = -0.5$ V vs NHE) for electron charging is less than that one can achieve under external electrical or electrochemical bias. Nevertheless, the electron equilibration experiments with photoirradiated TiO_2 colloids highlight our ability to obtain a quantitative estimate of the electron storage capacity of SWCNT bundles.

Charge Equilibration between SWCNT and TiO_2 Particles under UV Irradiation. To observe the electron equilibration between excited TiO_2 and SWCNT, we carried out UV irradiation ($\lambda > 300$ nm) of TiO_2 suspensions in the presence of SWCNT. Under these conditions, TiO_2 dominates the absorption of the incident UV light (see inset in Figure 2). The maximum absorbance at 650 nm was taken as a measure of electrons that accumulate within the TiO_2 particles. Figure 2 shows the change in absorbance with time at different levels of SWCNT concentrations. Two important observations emerge from this experiment. First, the saturation in the absorbance at 650 nm under steady-state illumination conditions is lower when SWCNT is present. It decreases with increasing concentration of SWCNT. Second, the time required to attain saturation in the absorbance is similar (~60 min) and is independent of SWCNT concentration. Once the electron equilibration is attained, any additional electrons generated in TiO_2 particles under UV excitation are lost in recombination. (The UV filtering effect caused by SWCNT is considered minimal. If internal filtering effect of light by SWCNT were a factor, we would have attained similar magnitude of absorbance saturation as we extend the photolysis for longer duration.)

Transient Absorption Studies. To probe the electron transfer between excited TiO_2 and SWCNT, we recorded
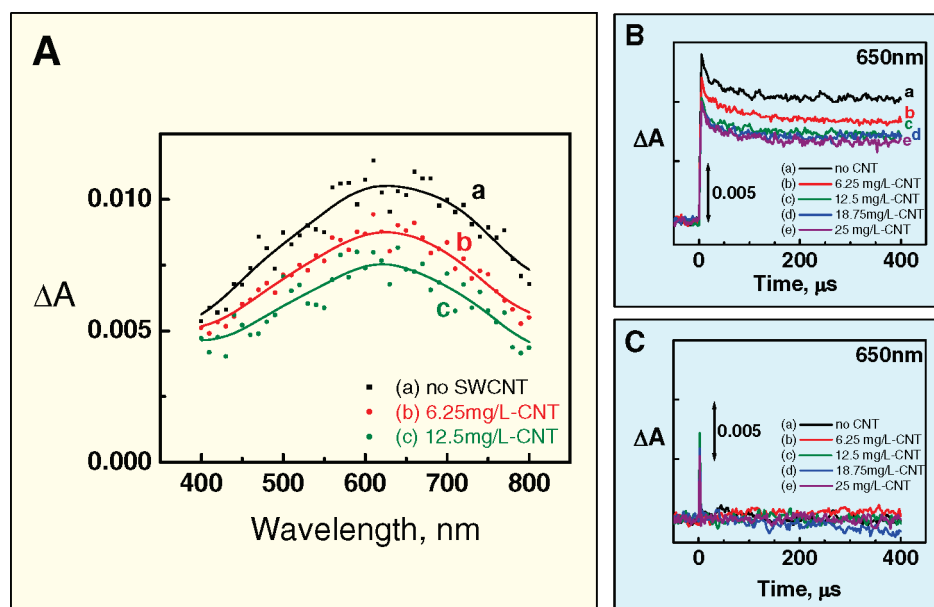

Figure 3. (A) Transient absorption spectra recorded 100 μs after 308 nm laser pulse excitation of 5.5 mM TiO_2 suspension in deaerated ethanol with (a) no SWCNT, (b) 6.25 mg/L SWCNT, and (c) 12.5 mg/L SWCNT. (B) Transient absorption–time profiles at 650 nm corresponding to the experiment in (A). (C) Transient absorption–time profiles at 650 nm in the absence of TiO_2.
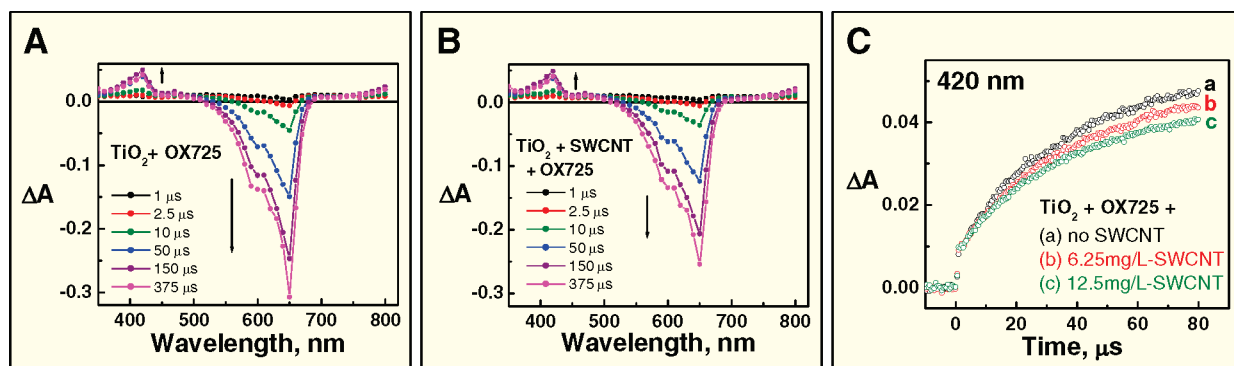
Figure 4. Time-resolved transient absorption spectra recorded following the 308 nm laser pulse excitation of 5.5 mM TiO_2 and 0.01 mM oxazine-725 in deaerated ethanol: (A) without and (B) with 6.25 mg/L SWCNT. (C) Absorption–time profiles recorded at 420 nm in the absence and presence of SWCNT.

transient absorption spectra following 308 nm laser pulse excitation (Figure 3A). In the absence of SWCNT the transient absorption spectrum exhibits spectral features (broad absorption maximum around 650 nm) similar to those observed in steady-state photolysis experiments. In the presence of SWCNT the magnitude of absorbance is lower, thus confirming the decreased electron accumulation in TiO_2 as a result of charge equilibration in the composite system. It should be noted that most of the 308 nm excitation is limited to TiO_2 nanoparticles, and the contribution of SWCNT to the overall absorbance at the excitation wavelength is relatively small. (The decrease in the transient absorbance observed in the presence of SWCNT is greater than can be accounted for by the competing absorption of incident light by the SWCNT.)

The prompt appearance of a transient absorption indicates that electron trapping is completed within the laser pulse duration of 10 ns. This time scale is in accordance with earlier observation that the electron trapping is completed within 30 ps.[46] The absorbance–time profiles shown in Figure 3B indicate that photogenerated electrons decay in the submillisecond time scale. The overall decay profile during this period is not significantly affected by the presence of SWCNT. However, the decrease in maximum absorbance observed in Figure 3B is an indication that the transfer of electrons to SWCNT occurs within the laser pulse duration ($\leq$10 ns). SWCNTs alone when excited with a 308 nm laser pulse do not exhibit any absorption in the microsecond time scale. It is important to employ lower laser intensity for excitation. At greater laser intensity (>5 mJ/pulse), artifacts arise and distort the transient signals. As shown in femtosecond transient absorption studies,[9,47] the photophysical events in SWCNT are ultrafast processes. Direct excitation of SWCNTs results in the formation of excitons, which in turn depletes the absorption in the visible region. The transient bleaching arising from SWCNT excitation quickly recovers as exciton recombination is completed within a few picoseconds.

Photoinduced Electron Transfer. We further probed the electron transfer property of TiO_2 and TiO_2–SWCNT sys-

tems by introducing an oxazine dye that is capable of accepting electrons following laser pulse excitation of TiO_2 and TiO_2–SWCNT composite systems. The dye, oxazine-725, is a useful probe for monitoring electron-transfer reactions in the microsecond time scale.[48] Because the triplet yield is negligible, it does not produce any detectable transients when subjected to nanosecond laser pulse excitation. The one-electron reduced form of the dye, on the other hand, exhibits absorption in the 420 nm region and thus facilitates monitoring of the electron-transfer product.[48] Figure 4A,B shows the transient absorption spectra following the 308 nm laser pulse excitation of TiO_2 and TiO_2–SWCNT suspensions containing oxazine-725. The reduction yield as monitored from the maximum absorbance at 420 nm or the disappearance of the ground-state dye (bleaching at 650 nm) is lower when SWCNT is present in the system. The absorption–time profiles at 420 nm (Figure 4C) show the time scale with which the electron transfer to the dye molecules occurs and redox equilibration is attained.

The commercially available SWCNTs used in the present experiments contain both metallic and semiconducting nanotubes with different chiralities. The energy gap of the SWCNT therefore ranges from 0 to 1.1 eV.[49] The reported work function of SWCNT bundles is about 4.8 eV versus absolute vacuum scale.[50] Charge transfer from the TiO_2 conduction band ($E_{CB} = -0.5$ V vs NHE) to the SWCNT conduction band ($E_{CB} \geq -0.3$ V vs NHE) is therefore energetically favorable for all types of SWCNTs. Earlier studies[4] carried out with CdS–SWCNT have shown that the electron transfer occurs with an average rate constant of 4×10^8 s^{-1}. Because of the charge equilibration between TiO_2 and SWCNT, we expect the Fermi level of the composite to be less negative than that of TiO_2, thus providing lower driving force for the overall reduction process.

On-Demand Discharge of Electrons Stored in SWCNT. If indeed the decreased electron accumulation and lower reduction yield observed with the TiO_2–SWCNT composite system arise from the charge equilibration process, we should be able to extract the electrons on de-

mand with another electron acceptor. To probe the charge transfer events as a stepwise reduction process, a TiO$_2$ particle suspension in ethanol (0.7 mL in a 2-mm path length quartz cell, deaerated and capped with a rubber septum) was first irradiated with UV light for 10 min. After attaining the absorbance of 0.04 at 650 nm, the UV irradiation was turned off. A known amount of deaerated thionine solution was added slowly in small increments using a microsyringe. The blue color of TiO$_2$ disappeared as the dye underwent reduction to form a stable leuco dye (Dye^{2-}, colorless product that remains stable in N$_2$ atmosphere) as illustrated by reactions 3 and 4.

$$TiO_2(e_t) + Dye \rightarrow TiO_2 + Dye^- \qquad (3)$$

$$2Dye^- \rightarrow Dye + Dye^{2-} \qquad (4)$$
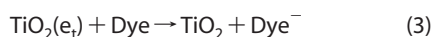
The negative absorption at 600 nm corresponding to the reduction of thionine indicates the electron transfer from TiO$_2$ to the dye. Once the electrons are titrated, further addition of thionine no longer results in absorption decrease at 600 nm. The point of addition at which one attains bleaching maximum represents the electron neutralization point.

Figure 5A shows the absorption changes recorded following the incremental addition of thionine dye to pre-irradiated TiO$_2$ suspension. The inset in Figure 5A shows the dependence of discharged electron concentration as estimated from the change in absorbance at 600 nm on the concentration of thionine dye. The break point in the titration curve corresponding to a thionine concentration of 132 μM indicates electron neutralization point. Because the disappearance of each thionine molecule represents two electrons, the titration value corresponds to 264 μM of electrons stored in the TiO$_2$ system. The dye molecules required to neutral-

ize electrons in the TiO$_2$ system thus provide a quantitative estimate of discharged electrons.

The above experiment was repeated using SWCNT in the TiO$_2$ system (Figure 5B). As described in the earlier section (Figure 1), the SWCNT suspension was first added to UV-irradiated TiO$_2$ suspension. The blue colored suspension becomes colorless as electrons are transferred from TiO$_2$ to SWCNT to attain charge equilibration. Addition of thionine to the equilibrated TiO$_2$–SWCNT composite suspension causes transfer of electrons from the composite to the dye, which in turn reflects a decrease in the absorption at 600 nm. The break point corresponding to the dye concentration of 96 μM shows the total number of extractable electrons from the composite (192 μM). In agreement with the earlier experiments, the reduction yield obtained with TiO$_2$–SWCNT composite is less than the value obtained in the absence of SWCNT (~73% of TiO$_2$ system). These stepwise reduction experiments further confirm the ability of SWCNT to accept electrons from TiO$_2$, store them under inert atmosphere, and discharge them to a redox couple on-demand.

Earlier studies have shown that the G-band of the resonance Raman spectrum of SWCNT bleaches as they are charged with electrochemical bias.[24,25] We also monitored the charging and discharging property of SWCNT film deposited on a conducting glass electrode using Raman spectroscopy. The TiO$_2$ particles were deposited on SWCNT film and irradiated with UV light in degassed ethanol solution. The Raman spectra were recorded after charging the film with photoirradiation and after exposing the system to ambient air (see Figure S3 in Supporting Information). As the stored electrons are scavenged by oxygen, we could restore the G-band in the Raman spectrum. The recovery of the Raman band confirms the ability of SWCNT to discharge stored electrons in air.
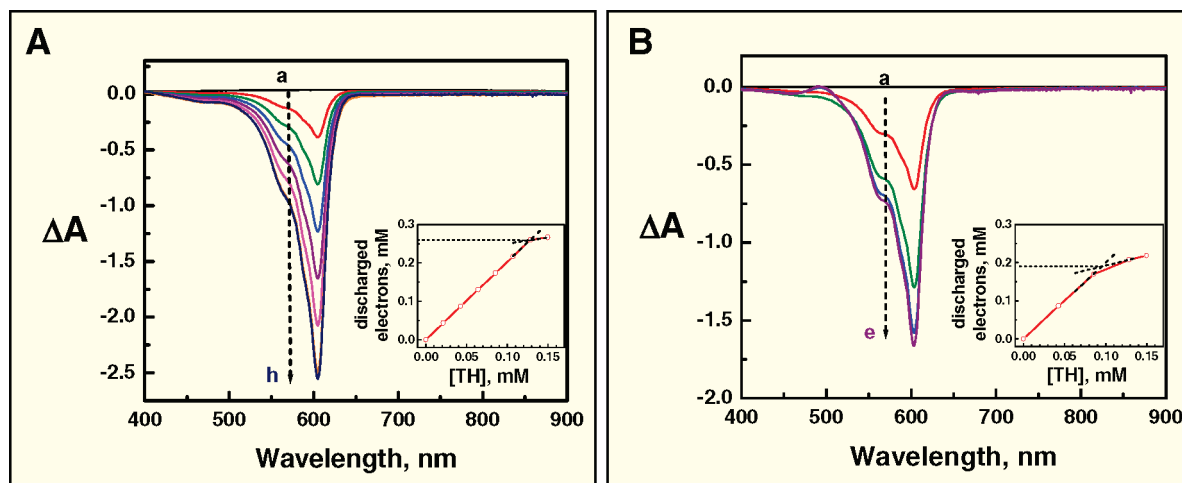

Figure 5. Changes in the absorption spectra following the addition of deaerated thionine solution to previously irradiated (A) TiO$_2$ and (B) TiO$_2$–SWCNT suspension in ethanol. A non-irradiated TiO$_2$ or TiO$_2$–SWCNT suspension was used as a reference. Insets show the concentrations of discharged electrons with each addition of thionine solution as estimated from the changes in the absorbance at 600 nm. The spectra recorded at each of these concentrations are presented in the absorption spectra a–h in (A) and a–e in (B).
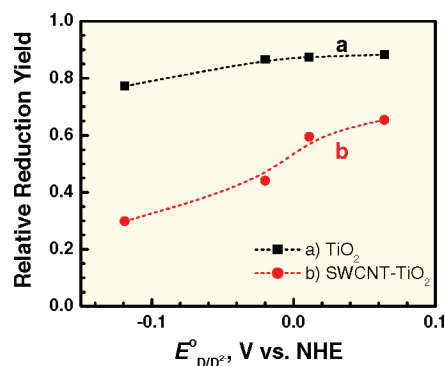
Figure 6. Dependence of relative reduction yield on the reduction potential of the dye for (a) TiO$_2$ and (b) TiO$_2$–SWCNT composite systems.

Steady-State Charge Equilibration with Dye Redox Couples. To probe the redox equilibration between the Dye^{2-}/Dye couple and TiO$_2$ (or TiO$_2$–SWCNT composite), we estimated the concentration of reduced dye and unreduced dye under equilibration conditions. We employed four different thiazine and oxazine dyes to estimate the transferable electrons stored in TiO$_2$ and TiO$_2$–SWCNT systems. The dyes chosen for this experiment have reduction potential ranging from -0.119 to $+0.064$ V versus NHE and are capable of accepting electrons from TiO$_2$ ($E_{CB} = -0.5$ V vs NHE). The procedure adapted here is similar to the one used to probe the Fermi level equilibration process between TiO$_2$ and Au system.[42]

A constant amount (150 μM) of dye solution was injected into the UV-irradiated TiO$_2$ and TiO$_2$–SWCNT composite suspensions under inert atmosphere. Only partial reduction of the dye occurred under these conditions. On the basis of the difference in the dye absorbance values, we were able to estimate the concentration of the reduced dye under equilibrium conditions in each of these experiments. Figure 6 shows the dependence of the reduction yield on the reduction potential of the dye. The dye, thionine, with its less negative reduction potential provides the maximum driving force for the electron transfer. These results establish the dependence of reduction yield on the dye reduction potential. The lower yield observed with TiO$_2$–SWCNT system is an indication that the driving force is lower compared to TiO$_2$ alone.

The Dye^{2-}/Dye redox couple in the above experiment exists in equilibrium with the Fermi level of TiO$_2$ and TiO$_2$–SWCNT composite. As shown previously,[42] we can employ a Nernst equation to determine the apparent Fermi level of TiO$_2$ (E_F^*) and TiO$_2$–SWCNT (E_F^{**}) system:
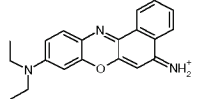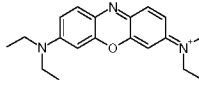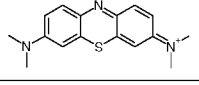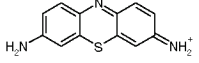
$$E_F^*(\text{TiO}_2(e)) = E_{fb} = E_{Ox/Red}^{\circ} + \frac{RT}{nF}\log\left(\frac{[\text{Ox}]_{eq}}{[\text{Red}]_{eq}}\right) \quad (5)$$

where E_{fb} is the flat band potential of TiO$_2$ (or TiO$_2$–SWCNT), $E_{Ox/Red}^{\circ}$ is the standard reduction potential of the redox couple, and n is the stoichiometric number of electrons involved in the reaction.

The analysis of charge equilibration experiments for four different dyes is summarized in Table 1. The conduction band of bulk TiO$_2$ is around -0.5 V NHE. In particulate systems the Fermi level remains less negative than the bulk conduction band as it equilibrates with the redox couple (Scheme 2). From Table 1 it is clear that the dye Nile Blue, with a more negative reduction potential, has the least driving force for the reduction process. Because of this smaller energy difference, we observe lower reduction yield for Nile Blue as compared to thionine. The equilibrated Fermi level measured for TiO$_2$–SWCNT is less negative than the corresponding value obtained with TiO$_2$ alone. Although the Fermi level shift observed for TiO$_2$–SWCNT is 20–30 mV, its influence on the overall reduction is significant, especially when the reduction potential of the acceptor is more negative (e.g., Nile Blue). Thus, the electron equilibration between SWCNT and TiO$_2$ should be taken into account when evaluating the photocatalytic activity of SWCNT-supported photocatalytic systems.

Implication of Charge Equilibration on the Photoelectrochemical Activity of Nanostructured TiO$_2$–SWCNT Films. We probed the effect of electron equilibration between TiO$_2$ and SWCNT on the photoelectrochemical effect in TiO$_2$ and TiO$_2$–SWCNT films.

TABLE 1. Charge Equilibration between Various Redox Couples and TiO$_2$ and TiO$_2$–SWCNT

Redox species	$E^{\circ}_{D/D^{2-}}$ V^a	TiO$_2$			TiO$_2$-SWCNT		
		$[D]_{eq}$ μM	$[D^{2-}]$ μM	E_F^* V^b	$[D]_{eq}$ μM	$[D^{2-}]$ μM	E_F^{**} V^b
Nile Blue A	-0.119	34.1	115.9	-0.135	105.3	44.7	-0.108
Oxazine725	-0.020	20.1	129.9	-0.044	83.9	66.1	-0.017
Methylene Blue	0.011	18.8	131.2	-0.014	60.8	89.3	0.006
Thionine	0.064	17.6	132.4	0.038	51.9	98.1	0.056

$^a E^{\circ}_{D/D^{2-}}$ were measured by cyclic voltammetry. ^{b}The apparent Fermi level was estimated using eq 5. All experiments were done under N$_2$ atmosphere using a 2-mm path length quartz cell. Total concentration of the dye added was same in all the experiments (150 μM). D and D^{2-} refer to Dye and Dye^{2-}, respectively.

The films of TiO₂ and TiO₂–SWCNT were deposited on the optically transparent electrodes (OTE) as described previously.[18] These films are photoactive and generate photocurrent under UV excitation when employed as photoanode in a photoelectrochemical cell. The primary process responsible for photocurrent generation is the charge separation in TiO_2 particles as they are subjected to bandgap ($E_g > 3.2$ eV) excitation.

Under open circuit conditions, the electrons accumulate and equilibrate with the redox couple in the electrolyte. The measured open circuit voltage is the difference between the apparent Fermi level of the semiconductor film and the reduction potential of the redox couple employed. Thus, the open circuit voltage is a direct measure of the apparent Fermi level of the semiconductor film if one equilibrates using the same redox couple. The photovoltage response of OTE/TiO₂ and OTE/SWCNT/TiO₂ electrodes (Figure 7) shows the increase in photovoltage in two steps. A prompt increase in the photovoltage is followed by a slow growth as the electrode equilibrates with the redox couple. Notably, the magnitude of the photovoltage was ~130 mV lower for the OTE/SWCNT/TiO₂ electrode as compared to that of the OTE/TiO₂ electrode. The lower photovoltage further supports the argument made in the previous section that the TiO₂–SWCNT composite has an apparent Fermi level lower than that of the pristine TiO₂ system. Similar to the charge equilibration effects in the suspension, the electrons are transferred from TiO₂ to SWCNT and thus attain a lower equilibrium potential.

In deaerated solution, the charges are retained within the film for a longer time. The photovoltage decay directly reflects the slow dissipation of accumulated electrons into the electrolyte as we stop the UV irradiation. It is interesting to note that the photovoltage decay of the OTE/SWCNT/TiO₂ electrode is slower than that of the OTE/TiO₂ electrode. This observation further ascertains the involvement of SWCNTs in the electron storage and equilibration process, thus increasing the survivability of accumulated electrons. Indeed, the ability of SWCNT to accept and transport electrons in the TiO₂–SWCNT film has shown its beneficial effect in the overall photocurrent generation.[18] A 2-fold increase of incident photon-to-photocurrent generation efficiency was achieved by employing a SWCNT conducting scaffold in TiO₂-nanostructure based photoelectrochemical cells.

The use of a SWCNT network as support architecture has its merit in facilitating transport of photogenerated electrons in light harvesting assemblies. However, electron equilibration and its influence on overall dynamics of the charge transfer process should be taken into account while designing hybrid architectures involving SWCNTs. Finally, it should also be noted that the electron storage and discharge properties of SWCNT reported in this study represent a general phenomenon based on a commercially obtained sample. It is likely that these properties are influenced by the chirality, di-
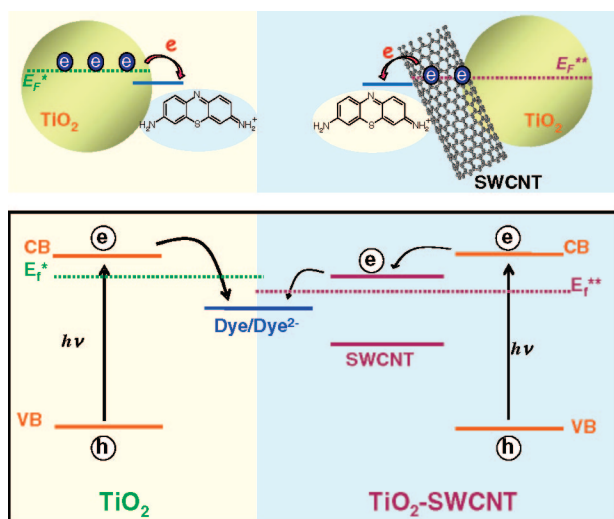
Scheme 2. Illustration of Fermi level equilibration of TiO₂ (left) and TiO₂–SWCNT (right) achieved in the presence of Dye/Dye²⁻ redox couple. Note the apparent Fermi level of TiO₂ (E_F^*) is less negative than TiO₂–SWCNT (E_F^{**}). Hence the energy difference ($E_F^{**} - E_{Dye/Dye^{2-}}$) is smaller than ($E_F^* - E_{Dye/Dye^{2-}}$).

ameter, and bundling effects. Further efforts are necessary to probe the effect of these individual parameters on the electron storage property.

CONCLUSIONS

Storage of 1 electron per 32 carbon atoms of SWCNTs has been achieved by bringing SWCNT in contact with photoirradiated semiconductor particles. These stored electrons can be discharged on demand using another electron acceptor. SWCNTs undergo charge equilibration with semiconductor particles such as TiO₂ and attain an apparent Fermi level more positive (20–30 mV in suspensions and 130 mV in films) than the Fermi level of semiconductor TiO₂. The ability of SWCNTs to accept electrons and transfer them to a suitable electron acceptor highlights the mediating role of these nanotubes in a charge transfer process. This electron-charging and -discharging property of SWCNT will play an important role in improving the performance of light energy harvesting applications.
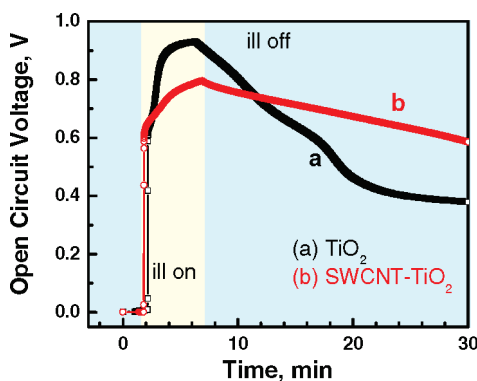

Figure 7. Photovoltage response of nanostructured films of TiO₂ and TiO₂–SWCNT films deposited on a conducting glass electrode during ON and OFF periods of illumination. Electrolyte was deaerated 1 M KOH, and the counter electrode was Pt.

EXPERIMENTAL SECTION

Reagent grade chemicals were purchased from Aldrich unless otherwise stated. Oxazine-725 and Nile Blue A dyes (laser grade) were obtained from Exciton. Methylene Blue (Fluka) was purified over a chromatography column of neutral alumina. The stock solution of TiO_2 colloids (0.05 M) was prepared by the hydrolysis of titanium isopropoxide in 0.1% acetic acid ethanol solution with constant stirring. The stock solution was allowed to age overnight and then diluted with ethanol to obtain 5.5 mM solution prior to use. The average particle diameter is in the range of 10–14 nm confirmed with an electron microscope.

SWCNT purchased from SES Research was first refluxed in 5 M HNO_3 solution for 1 h to remove any metal and organic impurities. The sample was subjected to repeated cycles of washing and centrifugation to remove excess acid. The SWCNT was solubilized in an organic solvent by sonication of dried SWCNT in tetrahydrofuran (THF) containing (~0.2 M) tetraoctylammonium bromide (TOAB).[51] Excess TOAB was removed by centrifugation, and the TOAB-bound SWCNTs were then suspended in a 0.005% Nafion ethanol solution to give a 0.5 mg/mL suspension of SWCNT. The commercially obtained sample is made up of 60–70% semiconducting SWCNTs.

In the steady-state experiments, photoexcitation of TiO_2 and TiO_2–SWCNT was carried out using collimated light from a 150 W xenon lamp filtered through a $CuSO_4$ solution ($\lambda > 300$ nm). Nanosecond laser flash photolysis experiments were performed using a Lambda Physik-Laser system (308 nm, output ~2.8 mJ/pulse, pulse width ~10 ns). The details of the experimental setup can be found elsewhere.[52] The experiments were performed in rectangular quartz cells with a probing length of 2 mm for the steady-state experiments and of 6 mm for the nanosecond laser flash photolysis experiments. All solutions were de-aerated with high-purity nitrogen. All experimentally determined values are within ±5% error.

For photoelectrochemical measurements, SWCNTs were assembled as a thin film on an optically transparent electrode (OTE, indium tin oxide conducting glass) using an electrophoretic deposition technique.[51] A known amount of TOAB-solubilized SWCNT suspension in THF (0.01 mg/ml) was transferred to a 1-cm cuvette in which two OTEs were kept at a distance of 4 mm. A dc voltage (60 V/cm) was applied between the electrodes, giving a SWCNT loading of 0.01 mg/cm^2 on the OTE. TiO_2 nanoparticles were deposited on the OTE/SWCNT (or OTE) from a suspension of TiO_2 power (Degussa P-25, mostly anatase) in 1% acetic acid methanol solution (5 mg/mL TiO_2) by drop casting. The TiO_2-modified electrodes were then annealed at 673 K in air for 30 min. The TiO_2 loadings were 2 mg/cm^2. Photoelectrochemical measurements were carried out in a conventional 3-arm electrochemical cell using Pt foil as the counter electrode and a standard calomel electrode as the reference electrode in a N_2-saturated 1 M KOH aqueous solution. A 100 W xenon lamp with a copper sulfate filter (>300 nm, 100 mW/cm^2) was employed for excitation of the photoelectrochemical cell.

Supporting Information Available: Details on the accumulation of electrons in photoexcited TiO_2 nanoparticles, estimation of electrons in TiO_2 by redox titration, and Raman spectra of charged SWCNT film. This material is available free of charge *via* the Internet at http://pubs.acs.org.

REFERENCES AND NOTES

1. Kamat, P. V. Meeting the Clean Energy Demand: Nanostructure Architectures for Solar Energy Conversion. *J. Phys. Chem. C* **2007**, *111*, 2834–2860.
2. Kamat, P. V. Harvesting Photons with Carbon Nanotubes. *Nanotoday* **2006**, *1*, 20–27.
3. Hasobe, T.; Fukuzumi, S.; Kamat, P. V. Organized Assemblies of Single-Wall Carbon Nanotube (SWCNT) and Porphyrin for Photochemical Solar Cells. Charge Injection from Excited Porphyrin into SWCNT. *J. Phys. Chem. B* **2006**, *110*, 25477–25484.
4. Robel, I.; Bunker, B.; Kamat, P. V. SWCNT–CdS Nanocomposite as Light Harvesting Assembly. Photoinduced charge transfer interactions. *Adv. Mater.* **2005**, *17*, 2458–2463.
5. Guldi, D. M.; Rahman, G. M. A.; Prato, M.; Jux, N.; Qin, S. H.; Ford, W. Single-Wall Carbon Nanotubes as Integrative Building Blocks for Solar-Energy Conversion. *Angew. Chem., Int. Ed.* **2005**, *44*, 2015–2018.
6. Hoppe, H.; Sariciftci, N. S. Organic Solar Cells: An Overview. *J. Mater. Res.* **2004**, *19*, 1924–1945.
7. Girishkumar, G.; Hall, T. D.; Vinodgopal, K.; Kamat, P. V. Single Wall Carbon Nanotube Supports for Portable Direct Methanol Fuel Cells. *J. Phys. Chem. B* **2006**, *110*, 107–114.
8. Kongkanand, A.; Kuwabata, S.; Girishkumar, G.; Kamat, P. Single-Wall Carbon Nanotubes Supported Platinum Nanoparticles with Improved Electrocatalytic Activity of Oxygen Reduction. *Langmuir* **2006**, *21*, 2392–2396.
9. Barazzouk, S.; Hotchandani, S.; Vinodgopal, K.; Kamat, P. V. Single Wall Carbon Nanotube Films for Photocurrent Generation. A Prompt Response to Visible Light Irradiation. *J. Phys. Chem. B* **2004**, *108*, 17015–17018.
10. Hasobe, T.; Fukuzumi, S.; Kamat, P. V. Stacked-Cup Carbon Nanotubes for Photoelectrochemical Solar Cells. *Angew. Chem., Int. Ed.* **2006**, *45*, 755–759.
11. Law, M.; Greene, L. E.; Johnson, J. C.; Saykally, R.; Yang, P. Nanowire Dye-Sensitized Solar Cells. *Nat. Mater.* **2005**, *4*, 455–459.
12. Adachi, M.; Murata, Y.; Okada, I.; Yoshikawa, S. Formation of titania nanotubes and applications for dye-sensitized solar cells. *J. Electrochem. Soc.* **2003**, *150*, G488–G493.
13. Galoppini, E.; Rochford, J.; Chen, H.; Saraf, G.; Lu, Y.; Hagfeldt, A.; Boschloo, G. Fast Electron Transport in Metal Organic Vapor Deposition Grown Dye-sensitized ZnO Nanorod Solar Cells. *J. Phys. Chem. B* **2006**, 16159–16161.
14. Mor, G. K.; Shankar, K.; Paulose, M.; Varghese, O. K.; Grimes, C. A. Use of Highly-Ordered TiO_2 Nanotube Arrays in Dye-Sensitized Solar Cells. *Nano Lett.* **2006**, *6*, 215–218.
15. Park, J. H.; Kim, S.; Bard, A. J. Novel carbon-doped TiO_2 Nanotube Arrays with High Aspect Ratios for Efficient Solar Water Splitting. *Nano Lett.* **2006**, *6*, 24–28.
16. Sirbuly, D. J.; Law, M.; Yan, H.; Yang, P. Semiconductor Nanowires for Subwavelength Photonics Integration. *J. Phys. Chem. B* **2005**, *109*, 15190–15213.
17. Klimov, V. I. Mechanisms for Photogeneration and Recombination of Multiexcitons in Semiconductor Nanocrystals: Implications for Lasing and Solar Energy Conversion. *J. Phys. Chem. B* **2006**, *110*, 16827–16845.
18. Kongkanand, A.; Domínguez, R. M.; Kamat, P. V. Single Wall Carbon Nanotube Scaffolds for Photoelectrochemical Solar Cells. Capture and Transport of Photogenerated Electrons. *Nano Lett.* **2007**, *7*, 676–680.
19. Frackowiak, E.; Beguin, F. Electrochemical Storage of Energy in Carbon Nanotubes and Nanostructured Carbons. *Carbon* **2002**, *40*, 1775–1787.
20. An, K. H.; Kim, W. S.; Park, Y. S.; Choi, Y. C.; Lee, S. M.; Chung, D. C.; Bae, D. J.; Lim, S. C.; Lee, Y. H. Supercapacitors using Single-Walled Carbon Nanotube Electrodes. *Adv. Mater.* **2001**, *13*, 497 +.
21. Futaba, D. N.; Hata, K.; Yamada, T.; Hiraoka, T.; Hayamizu, Y.; Kakudate, Y.; Tanaike, O.; Hatori, H.; Yumura, M.; Iijima, S. Shape-Engineerable and Highly Densely Packed Single-Walled Carbon Nanotubes and Their Application as Super-Capacitor Electrodes. *Nat. Mater.* **2006**, *5*, 987–994.
22. Kataura, H.; Kumazawa, Y.; Maniwa, Y.; Umezu, I.; Suzuki, S.; Ohtsuka, Y.; Achiba, Y. Optical Properties of Single-Wall Carbon Nanotubes. *Synth. Met.* **1999**, *103*, 2555–2558.
23. Petit, P.; Mathis, C.; Journet, C.; Bernier, P. Tuning and Monitoring the Electronic Structure of Carbon Nanotubes. *Chem. Phys. Lett.* **1999**, *305*, 370–374.
24. Kavan, L.; Rapta, P.; Dunsch, L. In Situ Raman and vis-NIR Spectroelectrochemistry at Single-Walled Carbon Nanotubes. *Chem. Phys. Lett.* **2000**, *328*, 363–368.
25. Kavan, L.; Rapta, P.; Dunsch, L.; Bronikowski, M. J.; Willis, P.;

Smalley, R. E. Electrochemical Tuning of Electronic Structure of Single-Walled Carbon Nanotubes: In-Situ Raman and vis-NIR Study. *J. Phys. Chem. B* **2001**, *105*, 10764–10771.

26. Kongkanand, A.; Kamat, P. V. Interactions of Single Wall Carbon Nanotubes with Methyl Viologen Radicals. Quantitative Estimation of Stored Electrons. *J. Phys. Chem. C* **2007**, *111*, 9012–9015.

27. Guldi, D. M.; Rahman, G. M. A.; Zerbetto, F.; Prato, M. Carbon Nanotubes in Electron Donor-Acceptor Nanocomposites. *Acc. Chem. Res.* **2005**, *38*, 871–878.

28. Chitta, R.; Sandanayaka, A. S. D.; Schumacher, A. L.; D'Souza, L.; Araki, Y.; Ito, O.; D'Souza, F. Donor-Acceptor Nanohybrids of Zinc Naphthalocyanine or Zinc Porphyrin Noncovalently Linked to Single-Wall Carbon Nanotubes for Photoinduced Electron Transfer. *J. Phys. Chem. C* **2007**, *111*, 6947–6955.

29. Hasobe, T.; Fukuzumi, S.; Kamat, P. V. Organized Assemblies of Single Wall Carbon Nanotubes and Porphyrin for Photochemical Solar Cells: Charge Injection from Excited Porphyrin into Single-Walled Carbon Nanotubes. *J. Phys. Chem. B* **2006**, *110*, 25477–25484.

30. Maruthamuthu, P.; Sharma, D. K.; Serpone, N. Subnano-second Relaxation Dynamics of 2,2′-Azinobis(3-ethylbenzo-thiazoline-6-sulfonate) and Chlorpromazine. Assessment of Photosensitization of a Wide Band Gap Metal Oxide Semiconductor TiO$_2$. *J. Phys. Chem.* **1995**, *99*, 3636–3642.

31. Kamat, P. V.; Bedja, I.; Hotchandani, S. Photoinduced Charge Transfer between Carbon and Semiconductor Clusters. One-Electron Reduction of C$_{60}$ in Colloidal TiO$_2$ Semiconductor Suspensions. *J. Phys. Chem.* **1994**, *98*, 9137–9142.

32. Warman, J. M.; de Haas, M. P.; Pichat, P.; Serpone, N. Effect of Isopropyl Alcohol on the Surface Localization and Recombination of Conduction-Band Electrons in Degussa P25 TiO$_2$. A Pulse-Radiolysis Time-Resolved Microwave Conductivity Study. *J. Phys. Chem.* **1991**, *95*, 8858–8861.

33. Fessenden, R. W.; Kamat, P. V. Rate constants for charge injection from excited sensitizer into SnO$_2$, ZnO, and TiO$_2$ semiconductor nanocrystallites. *J. Phys. Chem.* **1995**, *99*, 12902–12906.

34. Martin, S. T.; Herrmann, H.; Choi, W.; Hoffmann, M. R. Time Resolved Microwave Conductivity. Part 1. TiO$_2$ Photoreactivity and Size Quantization. *Faraday Trans.* **1994**, *90*, 3315–3322.

35. Graetzel, M.; Howe, R. F. Electron Paramagnetic Resonance Studies of Doped TiO$_2$ Colloids. *J. Phys. Chem.* **1990**, *94*, 2566–2572.

36. Howe, R. F.; Graetzel, M. EPR Observation of Trapped Electrons in Colloidal TiO$_2$. *J. Phys. Chem.* **1985**, *89*, 4495–4499.

37. Rajh, T.; Ostafin, A. E.; Micic, O. I.; Tiede, D. M.; Thurnauer, M. C. Surface Modification of Small Particle TiO2 Colloids with Cysteine for Enhanced Photochemical Reduction. An EPR Study. *J. Phys. Chem.* **1996**, *100*, 4538–4545.

38. Rothenberger, G.; Moser, J.; Graetzel, M.; Serpone, N.; Sharma, D. K. Charge Carrier Trapping and Recombination Dynamics in Small Semiconductor Particles. *J. Am. Chem. Soc.* **1985**, *107*, 8054–8059.

39. Kamat, P. V.; Ford, W. E. Photochemistry on Surfaces: Triplet-Triplet Energy Transfer on Colloidal TiO$_2$ Particles. *Chem. Phys. Lett.* **1987**, *135*, 421–6.

40. Kamat, P. V. Photochemistry on Nonreactive and Reactive (Semiconductor) Surfaces. *Chem. Rev.* **1993**, *93*, 267–300.

41. Jakob, M.; Levanon, H.; Kamat, P. V. Charge Distribution between UV-Irradiated TiO$_2$ and Gold Nanoparticles. Determination of Shift in Fermi Level. *Nano Lett.* **2003**, *3*, 353–358.

42. Subramanian, V.; Wolf, E. E.; Kamat, P. V. Catalysis with TiO$_2$/Au Nanocomposites. Effect of Metal Particle Size on the Fermi Level Equilibration. *J. Am. Chem. Soc.* **2004**, *126*, 4943–4950.

43. An, K. H.; Kim, W. S.; Park, Y. S.; Moon, J. M.; Bae, D. J.; Lim, S. C.; Lee, Y. S.; Lee, Y. H. Electrochemical Properties of High-Power Supercapacitors using Single-Walled Carbon Nanotube Electrodes. *Adv. Funct. Mater.* **2001**, *11*, 387–392.

44. Gao, B.; Bower, C.; Lorentzen, J. D.; Fleming, L.; Kleinhammes, A.; Tang, X. P.; McNeil, L. E.; Wu, Y.; Zhou, O. Enhanced Saturation Lithium Composition in Ball-Milled Single-Walled Carbon Nanotubes. *Chem. Phys. Lett.* **2000**, *327*, 69–75.

45. Zhao, J.; Buldum, A.; Han, J.; Lu, J. P. First-Principles Study of Li-Intercalated Carbon Nanotube Ropes. *Phys. Rev. Lett.* **2000**, *85*, 1706–1709.

46. Serpone, N.; Lawless, D.; Khairutdinov, R.; Pelizzetti, E. Subnanosecond Relaxation Dynamics in TiO$_2$ Colloidal Sols (Particle Sizes R_p = 1–13.4 nm). Relevance to Heterogeneous Photocatalysis. *J. Phys. Chem.* **1995**, *99*, 16655–16661.

47. Ma, Y. Z.; Stenger, J.; Zimmermann, J.; Bachilo, S. M.; Smalley, R. E.; Weisman, R. B.; Fleming, G. R. Ultrafast Carrier Dynamics in Single-Walled Carbon Nanotubes Probed by femtosecond Spectroscopy. *J. Chem. Phys.* **2004**, *120*, 3368–3373.

48. Kamat, P. V. Photoelectrochemistry in Particulate Systems. 3. Phototransformations in the Colloidal TiO$_2$-Thiocyanate System. *Langmuir* **1985**, *1*, 608–11.

49. Sun, G. Y.; Kurti, J.; Kertesz, M.; Baughman, R. H. Variations of the Geometries and Band Gaps of Single-Walled Carbon Nanotubes and the Effect of Charge Injection. *J. Phys. Chem. B* **2003**, *107*, 6924–6931.

50. Suzuki, S.; Bower, C.; Watanabe, Y.; Zhou, O. Work Functions and Valence Band States of Pristine and Cs-Intercalated Single-Walled Carbon Nanotube Bundles. *Appl. Phys. Lett.* **2000**, *76*, 4007–4009.

51. Kamat, P. V.; Thomas, K. G.; Barazzouk, S.; Girishkumar, G.; Vinodgopal, K.; Meisel, D. Self-Assembled Linear Bundles of Single Wall Carbon Nanotubes and Their Alignment and Deposition as a Film in a DC-Field. *J. Am. Chem. Soc.* **2004**, *126*, 10757–10762.

52. Thomas, M. D.; Hug, G. L. A Computer-Controlled Nano-second Laser System. *Comput. Chem. (Oxford)* **1998**, *22*, 491–498.